Response to reviewer 2.

We thank Patrick Chuang for the detailed and very helpful comments, which have significantly improved the presentation of the manuscript. A point-by-point response to the reviewer's comments is listed below.

Main comment: ***My one major comment is that, common to many studies of this type, the comparisons of observations with the LES simulations are not quantitative…***

We agree with the reviewer that evaluation of LES simulations should be more quantitative in general as a rigorous evaluation is crucial to improving current LES technique including subgrid-scale representations. To address the reviewer's concern, we have added the turbulence leg averages for mean$\theta_l$, $q_t$, $u$, and $v$ and the 3rd-moment $\overline{w'^3}$ in Fig. 3 for more comparison (see attached figure). Thus, there are now in total 4 mean and 5 turbulence variables from observations for comparison with LES results. In addition, to add more quantitative comparison, the cloud-layer averages of the mean and turbulence variables are calculated and listed in Table 2 (see attached table). We have tried to use observations as much as possible in the comparison analysis in the study.

One of the issues for a more rigorous quantitative turbulence comparison in this study is that there are only 6 horizontal leg levels and each leg is only 10 minutes long for this flight. Therefore, it is difficult to obtain meaningful turbulence statistics by further splitting a leg into smaller segments for error analysis. In addition, the observed turbulence profiles are not very complete. Remote sensing measurements offer more complete turbulence profiles such as the $w$ variance, thus may provide better data for more rigorous quantitative evaluation. The objective of the LES comparison with observations in this study is to make sure that the simulated MBL structure is consistent with the observations so that investigation can be carried out. We think we have achieved this objective.

We have included the following statement regarding to the comparison near the end of section 3.

"To provide more comparison, the LES results and observations are averaged using values at the aircraft turbulence-leg levels within the cloud layer; they are presented in Table 2. As shown in Fig. 3 and Table 2, The SS simulated MBL compares better than the others in terms of the mean thermal profiles and the main 2nd-moment turbulence variables such as $\overline{w'^2}$, $\rho_0 C_p \overline{w'\theta_v'}$ and the total momentum flux. This is expected as the shear forcing for SS resembles the reality more closely than that for either WS or NS."

p. 4946, line 20, "the" is included before MBL.

47, 17: Wrong unit for $q_c$ is corrected.

48, 3-4: ***I'm not sure what "directly controlled" means since a few sentences later….***

The clause “directly controlled by ..” is removed.

48, 10-13: We agree; the sentence is moved.

49, 7: Fixed.

49, 11: ***Needs more explanation? It’s not clear to me why change in the mean radiative ….***

The negative distribution of the turbulence field is caused by the negatively buoyant downdrafts driven by both the radiative and evaporative cooling. Both Nicholls (1989) and Yamaguchi and Randall (2012) discuss in detail how downdrafts are driven by the radiative and evaporative cooling, even though their relative emphasis is different. Because the cloud-top radiative cooling provides the fundamental source of the thermal instability for the stratocumulus convection, a larger mean radiative cooling results in a stronger convective circulation with stronger downdrafts and updrafts, leading to a lager negative $\overline{w'^3}$.

We rewrite this part as follows.

“Golaz et al (2005) analyzed $\overline{w'^3}$ budget using LES simulations; they concluded that negatively skewed *w* field in stratocumulus clouds is caused by the negatively buoyant downdrafts that are driven by the radiative as well as evaporative cooling (Nicholls, 1989; and Yamaguchi and Randall, 2012). For NS, the large liquid water results in strong radiative cooling, leading to larger negative values of $\overline{w'^3}$.”

49, 12: ***“It may be also...” This is not well-explained - ….***

This part is rewritten. See previous comment.

49, 15: ***“For all three w fields...” It’s not clear this is true for the SS case…***

The averaged updraft/downdraft characteristics are calculated and presented in Fig. 4 to demonstrate that a narrower downdraft fractional area is associated with stronger downdrafts and weaker updrafts.

50, 22***. Can you mark z_itop and z_ibase levels on the profiles in Fig. 5?***

These levels ($z_{itop}$ and $z_{ibase}$) are marked in Fig. 5.

51,5-14***. Fig 6d shows around 8h, the shear in the WS cases crosses over …***

We thank the reviewer for pointing out the crossover of the shear curves for the SS and WS cases. The discussion about Fig. 6 is rewritten. We want to emphasize that the controlling parameter is the Richardson number, not the shear. Because we are examining overall characteristics of the inversion with Fig. 5, we focus on the bulk Richardson number [Eq. (2)]. The thickness of the inversion layer is strongly regulated by $Ri_b$. The shear has an impact

mainly through $Ri_b$. Particularly, when $Ri_b$ is close to the equilibrium number (~0.3 for the SS case), the thickness increases significantly as the turbulence intensity gets much stronger as in the case of SS. To reflect our emphasis on the overall forcing of the inversion flow, we replace the mean shear term with the overall shear in Fig. 6e (see attached figure), which shows a larger overall shear in SS than in WS. We have added the following paragraph discussing the stronger mean shear in WS. For WS, $Ri_b$ is still above 0.5 even though the mean shear is stronger, because the stability effect still dominates due to the very thin inversion layer. The inversion thickness from WS is greater than that from NS and less than in SS as the value of the WS $Ri_b$ is between the SS and NS simulations

"It is interesting to note that the mean shear of WS across the inversion ( $SH = \sqrt{(\Delta\overline{u})^2 + (\Delta\overline{v})^2} / \Delta z_i \approx 0.012$ ) is actually greater than that of SS ($SH \approx 0.01$) for last 1.5 hours, even though the overall shear of SS is significantly stronger as shown in Fig. 6d. It occurs because the shear of WS is concentrated within a considerably thinner $\Delta z_i$ under the weak shear forcing such that the mean thermal stability ($\Delta\overline{\theta_{vl}}/\Delta z_i$) dominates the shear in terms of $Ri_b$, whose value is larger for WS than that for SS. Therefore, it is the bulk or gradient Richardson number that has a more fundamental control of the turbulent mixing within the inversion layer."

51, 20-11. ***"In fact..." This is simply the discretization of z, right?*** …..

It is important that $Ri_b$ increases with the increase in $\Delta z_i$, because it suggests an adjustment of the stability in the process. Since both reviewers have similar comments, we simply remove this sentence and rewrite: "It is noteworthy that $Ri_b$ of SS decreases, but tends to stay slightly above 0.3 for last 3 hours despite an increase in the overall wind shear $\sqrt{(\Delta\overline{u})^2 + (\Delta\overline{v})^2}$ (Fig. 6d) and $\Delta z_i$."

51, 24: ***Fig 6e (and also the next sentence) say that shear decreases over time,*** …
Our statements were indeed confusing, and they are removed in the revised manuscript. The revised paragraph is as follows.

"These results suggest that there exists a feedback mechanism between the large-scale conditions and turbulence mixing through the inversion stability. The large-scale subsidence and radiative cooling near the cloud top tends to create a sharp inversion with a strong dynamic stability, whereas wind shear acts to destabilize the inversion. When the shear is sufficiently intense such that $Ri_b$ (or $Ri$) approaches the critical value (e.g., 0.25), the turbulence is significantly enhanced with an increased $\Delta z_i$, leading to a slightly larger $Ri_b$ (or $Ri$). Eventually, an equilibrium $Ri_b$ (or $Ri$) is reached. Through this process, the MBL height increases with a thicker inversion layer."

52, 14***. "three levels within..." I don't quite understand how the levels were chosen***.

We have included more explanations on how the three levels are chosen. Because a cloud-free sublayer is present within the inversion layer for each of the cases¸ we specifically chose a level within this sublayer for each case for the PDF analysis. These levels are chosen by examining

the temperature and cloud fraction profiles (Fig. 7b and c); they are marked in Fig. 7b. Since these levels are all in the upper part of the inversion layer and also cloud free, the comparison at these levels is justified. It is understood that PDF of the instantaneous local Richardson number $Ri_l$ may strongly depend on the level chosen as indicated by the *Ri* profiles shown in Fig, 5c. Fig. 7a and Fig 8 provide an example that illustrates how turbulence is controlled by *Ri* in the cloud-free sublayer.

If the exact level is changed, the $Ri_l$ PDF will be different. However, the mean value and the standard deviation from the SS PDF are always smaller than those from WS. Since there is vertical variation in the Richardson number in the cloud-free sublayer (particularly for WS), it is not justified for PDF to include all grid points at all levels in the sublayer. It is likely the results will be different if all the sublayer grid points are included.

52, 15: ***In my copy, there's no curve for the NS condition in Fig 7a…..***

The PDF of NS is removed from Fig. 7a; it is explained in text.

54, 20. ***"This is a departure ..." This doesn't seem totally true to my eye at least***

This sentence has been reworded. The new statement is, "The buoyancy flux minimum just below clouds decreases in this weakening process and approaches zero in SSN compared to 17 $Wm^{-2}$ from NSN. This difference in the minimum values between SSN and NSN is significantly larger than that between SS and NS (Fig. 3f), suggesting that the solar warming has in part concealed the shear effect in the cloud layer."

55, 4***. Change Fig 9e to plot radiative heating like in Fig 3f – no reason for the inconsistency and heating rates are easier to interpret.***

The reason for radiative flux and $\rho_0 C_p \overline{w'\theta_l'}$ in Fig. 9d and e is that we are discussing mixed-layer heat budget here, for which total radiative flux divergence in the MBL is more relevant than the cooling rate near the top of the MBL. The flux profiles give an idea of magnitudes of these divergences. Note that the total divergence is also included in Table 2. Therefore, we feel that the flux profiles are more informative in Fig. 9, and therefore keep them in the figure.

58, 1: ***"zero just below clouds". "zero just below clouds" Doesn't this demonstrate fairly strong…..***

By "weak", we mean that the cloudiness does not decrease even though the nonlinearity in the moisture flux is clearly present (Fig. 9c). But we agree with the reviewer that the term "weak" may introduce some confusion to readers. Therefore, we have removed "weak" in this and other relevant statements.

Fig. 3: ***needs a different title,***

Title is changed to “LES simulated and observationally derived mean and turbulence variables”. More measurements are added in these plots. The labels are redone to reflect the turbulent fluctuations.

Fig. 5: ***all panels are missing the “primes” on the x-axis labels.***

Labels are corrected.

Table 2. Comparison between LES and observation results averaged in the cloud

| Cloud Layer Avg. | $\overline{\theta_l}$ K | $\overline{q_t}$ g kg$^{-1}$ | $\overline{q_c}$ g kg$^{-1}$ | $\bar{u}$ m s$^{-1}$ | $\bar{v}$ m s$^{-1}$ | $\overline{w'^2}$ m$^2$s$^{-2}$ | $\overline{w'\theta_v'}$ W m$^{-2}$ | $\overline{w'^3}$ m$^3$ s$^{-3}$ | Stress N m$^{-2}$ | $\overline{w'q_t'}$ W m$^{-2}$ |
|---|---|---|---|---|---|---|---|---|---|---|
| OBS | 290.5 | 7.86 | 0.09 | 0.4 | -2.0 | 0.1 | 3 | -0. 017 | 0.02 | 8.0 |
| SS | 290.2 | 7.87 | 0.15 | 5.1 | -0.5 | 0.09 | 4.2 | -0.005 | 0.03 | 21.8 |
| WS | 290.0 | 7.98 | 0.23 | 2.5 | 0.9 | 0.11 | 8.8 | -0.013 | 0.015 | 21.3 |
| NS | 289.9 | 7.98 | 0.27 | 0 | 0.0 | 0.14 | 11.2 | -0.020 | 0.004 | 17.3 |

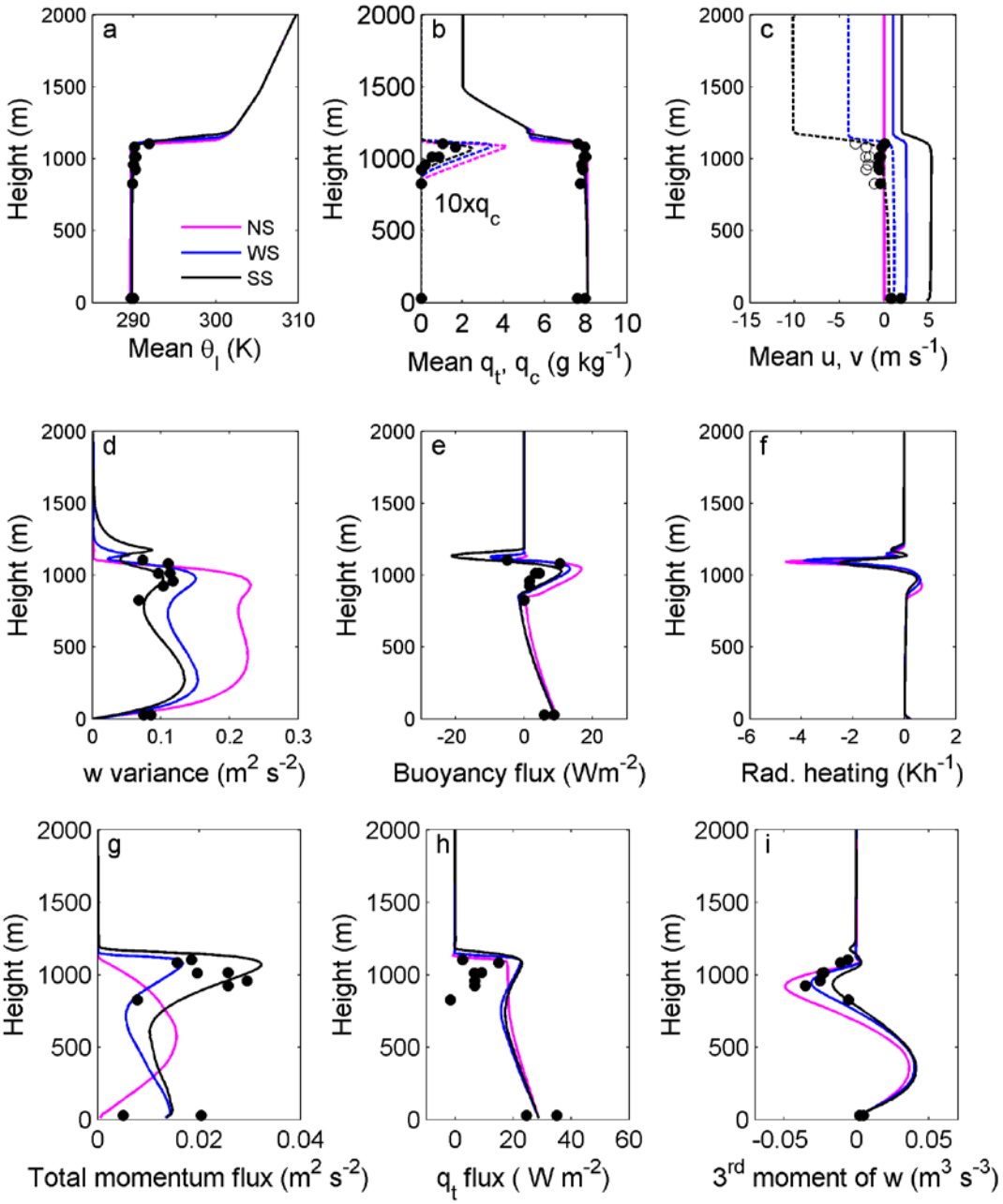


Fig. 3. LES simulated and observationally derived mean and turbulence variables. Solid or dashed lines denote the simulated results; the circles are the leg averaged values derived from measurements. (a) $\overline{\boldsymbol{\theta}_{\boldsymbol{l}}}$; (b) $\overline{\boldsymbol{q}_{\boldsymbol{t}}}$ or $\overline{\boldsymbol{q}_{\boldsymbol{c}}}$; (c) $\overline{\boldsymbol{u}}$ (solid) and $\overline{\boldsymbol{v}}$ (dashed), the solid and open circles are for observed $\overline{\boldsymbol{u}}$ and $\overline{\boldsymbol{v}}$, respectively.; (d) $\overline{\boldsymbol{w'^2}}$; (e) $C_p\rho_0\,\overline{w'\theta_v'}$; (f) radiative heating rate; (g) total momentum flux; (h) $L\rho_0\,\overline{w'q_t'}$; (i) $\overline{w'^3}$.

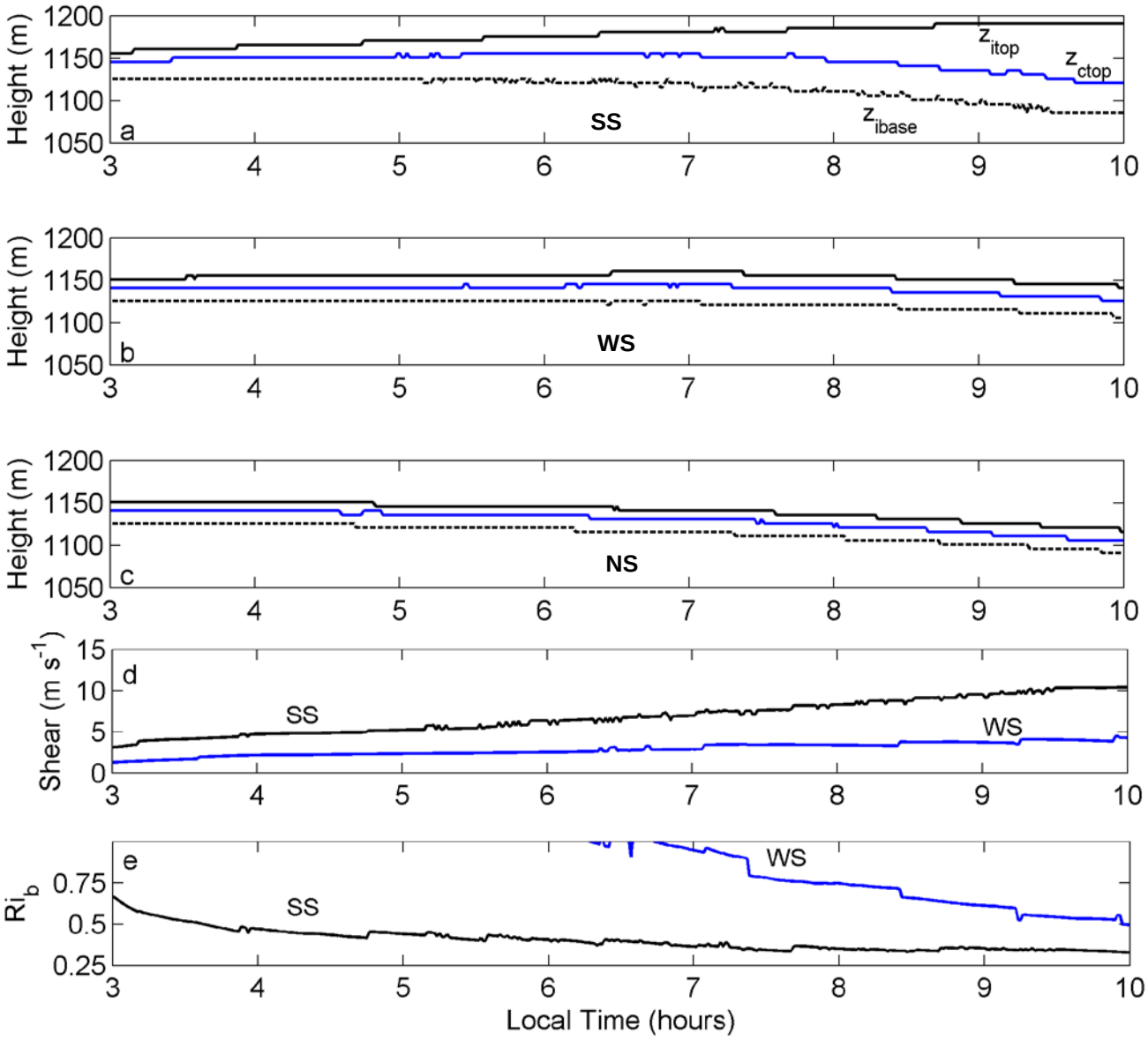


Fig. 6: Temporal evolutions of the inversion layer characteristics. (a) – (c) Evolution of the inversion top $z_{itop}$ (solid black curve), inversion base $z_{ibase}$ (dashed black) and cloud-top heights $z_{ctop}$ (blue lines); (d) the overall wind shear ( $\sqrt{(\Delta\bar{u})^2 + (\Delta\bar{v})^2}$ ) with black curve for SS and blue for WS; and (e) the bulk Richardson number $Ri_b$ with the black for SS and blue for WS. The wind shear from NS is zero and $Ri_b$ is ill-defined; they are not presented here.